Science in China Series C: Life Sciences

www.scichina.com
life.scichina.com
www.springerlink.com

Liver X receptor agonist T0901317 reduces atherosclerotic lesions in *apoE*$^{-/-}$ mice by up-regulating *NPC1* expression

OU Xiang[1,2*], DAI XiaoYan[1*], LONG ZhiFeng[3], TANG YaLing[1], CAO DongLi[1], HAO XinRui[1], HU YanWei[1], LI XiaoXu[1] & TANG ChaoKe[1†]

[1] Institute of Cardiovascular Research, Key Laboratory for Atherosclerology of Hunan Province, University of South China, Hengyang 421001, China;
[2] Department of Physiology, Medical College of Shaoguan University, Shaoguan 512026, China;
[3] Department of Histology and Embryology, University of South China, Hengyang 421001, China

In this study, we studied the effect of liver X receptor (LXR) agonist T0901317 on Niemann-Pick C1 protein (NPC1) expression in *apoE*$^{-/-}$ mice. Male *apoE*$^{-/-}$ mice were randomized into 4 groups, baseline group (*n*=10), control group (*n*=14), treatment group (*n*=14) and prevention group (*n*=14). All of the mice were fed with a high-fat/high-cholesterol (HFHC) diet containing 15% fat and 0.25% cholesterol. The baseline group treated with vehicle was sacrificed after 8 weeks of the diet. The control group and the prevention group were treated with either vehicle or T0901317 daily by oral gavage for 14 weeks. The treatment group was treated with vehicle for 8 weeks, and then was treated with the agonist T0901317 for additional 6 weeks. Gene and protein expression was analyzed by real-time quantitative PCR, immunohistochemistry and Western blotting, respectively. Plasma lipid concentrations were measured by commercially enzymatic methods. We used RNA interference technology to silence *NPC1* gene expression in THP-1 macrophage-derived foam cells and then detected the effect of LXR agonist T0901317 on cholesterol efflux. Plasma triglyceride (TG), total cholesterol (TC), high density lipoprotein cholesterol (HDL-C) and apoA-I concentrations were markedly increased in T0901317-treated groups. T0901317 treatment reduced the aortic atherosclerotic lesion area by 64.2% in the prevention group and 58.3% in the treatment group. LXR agonist treatment increased *NPC1* mRNA expression and protein levels in the small intestine, liver and aorta of *apoE*$^{-/-}$ mice. Compared with the normal cells, cholesterol efflux of siRNA THP-1 macrophage-derived foam cells was significantly decreased, whereas cholesterol efflux of LXR agonist T0901317-treated THP-1 macrophage-derived foam cells was significantly increased. Our results suggest that LXR agonist T0901317 inhibits atherosclerosis development in *apoE*$^{-/-}$ mice, which is related to up-regulating *NPC1* expression.

Niemann-Pick C1 protein, liver X receptor agonist, atherosclerosis, plaque

Monocytes migrate into the blood vessel endothelium space and differentiate into macrophages. Macrophages turn into foam cells after acquiring a mass of lipoprotein-derived cholesterol[1]. Cholesterol accumulation in macrophage-derived foam cells is one of the important events of atherogenesis[2]. Mobilization to the plasma membrane and efflux to extracellular acceptors of intracellular cholesterol are important mechanisms of cells in regulating the cholesterol level. This is the first step of reverse cholesterol transport (RCT).

Niemann-Pick disease type C (NPC) is a fatal auto-

Received September 26, 2007; accepted December 12, 2007
doi: 10.1007/s11427-008-0054-4
†Corresponding author (email: tchaoke@yahoo.com.cn)
* These authors contributed equally to this study
Supported by the National Natural Science Foundation of China (Grant No. 30470720) and Hunan Provincial Natural Sciences Foundation of China (Grant No. 06jj5058)

somal recessive lipid storage disorder characterized by lysosomal accumulation of cholesterols and gangliosides[3], caused by mutations in *NPC1* or Niemann-Pick C2 protein (NPC2)[4,5]. Mutations in *NPC1* account for 95% of all of the NPC cases, whereas mutations at NPC2 account for the remaining 5%[6]. *NPC1* is expressed in almost every tissue[7] and researched widely at the cellular and molecular level.

NPC1 gene of human and mouse has been identified by positional cloning methods[8]. *NPC1* is expressed in gene spanning more than 47 kb and contains 25 exons[9]. NPC1 is a transmembrane glycoprotein localized in the late endosomal compartment with a sterol-sensing domain projected into the lumen[10] and supervises the change of the cellular cholesterol level and regulates the intracellular lipid homeostasis by altering the manner of vesicle transport or participating in lipid transmembrane transportation directly. NPC2 is a soluble cholesterol-binding protein localized in the lysosome[11]. NPC1 and NPC2 control cholesterol trafficking to the plasma membrane[12].

The livers X receptors (LXRs) are ligand-dependent transcription factors belonging to the nuclear hormone receptor superfamily, and they can regulate the expression of genes controlling lipid metabolism[13]. In small intestine, LXR can control sterol absorption by regulating expression of ATP-binding cassette transporter A1 (ABCA1), ABCG5 and ABCG8[14]. In macrophages, LXR ligands enhance apoA-I-mediated cholesterol efflux through up-regulating ABCA1 expression[15]. The natural ligands for LXR include oxidized derivatives of cholesterol, such as 22(R)-hydroxycholesterol and 27-hydroxycholesterol[16]. T0901317 is a synthetic LXR activator broadly used for the research in LXR biology[17]. It is well known to similar efficacy to natural ligands, but it is significantly more potent and selectively bound to LXR[18].

Recent research has shown that LXR agonists can enhance the mobilization of free cholesterol to the plasma membrane by inducing *NPC1* and *NPC2* gene expression in macrophages, resulting in enriched cholesterol content in the outer layer of the plasma membrane, thus becoming more available for efflux[12]. Because 95% of NPC cases are caused by *NPC1* mutation, it is obvious that the role of NPC1 in intracellular lipid trafficking is much greater than that of NPC2. Furthermore, the effect of LXR agonists on *NPC1* expression *in vivo* has not been clarified. In this study, we fed *apoE*$^{-/-}$ mice with a high-fat/high-cholesterol (HFHC) diet with a synthetic nonoxysterol LXR agonist T0901317 and observed the influence of T0901317 on *NPC1* expression and atherosclerotic lesions in the *apoE*$^{-/-}$ mice. In addition, we explore the role of NPC1 in atherosclerosis initiation and development by investigating the influence of T0901317 on intracellular cholesterol efflux in *NPC1* gene-silenced THP-1 macrophage-derived foam cells.

1 Materials and methods

1.1 Animals and diets

Male 8-week-old *apoE*$^{-/-}$ mice and HFHC diet were purchased from Laboratory Animal Center of Peking University, China.

1.2 Materials

T0901317 was obtained in Cayman Chemical and dissolved in vehicle (PEG400: Tween 80, 4:1), stored at –20℃. Goat-anti-mouse NPC1 antibody and horseradish peroxidase (HRP)-conjugated rabbit-anti-goat antibody were purchased from Santa Cruz Biotechnology, Inc. Western Blotting Luminol Reagent (sc-2048) was obtained from Zhongshan Golden Bridge Company. The BCA protein assay kit and Blue Ranger prestained protein molecular mass marker mix were provided by Hyclone-Pierce. Ponceau S staining solution and Poly-L-Lysine Solution were from Sigma Company. Streptavidin-biotin-peroxidase (SABC-AP) kit was obtained from Boster Bioengineering Company. DyNAmoTM SYBR Green qPCR kit was bought from Finnish Finnzymes Company. RevertAidTM First Strand cDNA Synthesis Kit (#k1622) was purchased from Fermentas. Pentobarbital sodium and neutral balsam were gained from Shanghai Chemistry Reagent Company in China National Group of Medicines. Pentobarbital sodium was dissolved in deionized water to turn into 1% solution, filtered through a filter membrane to get rid of bacteria and stored at room temperature. TRIzol reagent is the production of BBI Company, Canada. DEPC came from Amersco Company, USA. PSilencer2.1-U6-Hygro was obtained from Ambion Company. LipofectamineTM 2000 was from Invitrogen Company. Other chemicals were commercially available.

1.3 Main apparatuses and equipments

Automatic biochemical analysor (CX717) was the production of Hitachi Company, Japan. Vacuum tissue

processor (TSJ-III) paraffin embedding apparatus (BMJ-III) and pathohistological tissue embedding/cooling desk (BMJ-III) were the productions of Changzhou Zhongwei Electronic Instruments Plant, China. Slicing cutter (325) came from Thermo Shandon Corporation, USA. Assembly equipment (HI1210) was from Leica Company, Germany. Biological microscope (BX51) was the production of Olympus Company, Japan. Image Analysis System (HMIAS2000) was the production of Qianping Image Technology Limited Liability Company. High speed centrifuge (5084/5084R) was from Eppendorf Corporation, Germany. Ultraviolet-visible spectrophotometer (Lambda25) was the production of PE Company, USA. Electronic analytical balance was from Sartorius Company, USA. Micropipettors (10, 100, 1000 μL) were from Eppendorf Corporation, Germany. Silicone rubber pipe of 0.3 mm in internal diameter came from Dow Corning Corporation, USA. 25.4 mm×76.2 mm ground glass slide (7105) and 18 mm×18 mm coverslip (7201) were the production of Changlong Apparatus Limited Company of Haimen, China. Paraffin wax was from Sample Model Plant of Shanghai, China. Real-time quantitative PCR was performed on an Applied Biosystems 7900HT Fast Real-Time PCR System. Polyacrylamide gel ele- ctrophoresis chamber was the production of BIO-RAD Company, USA. Semidry Transfer System was from Wealtec Company, USA.

1.4 Preparation of animal model

Male 8-week-old *apoE*$^{-/-}$ mice were bred in the SPF Animal Laboratory and fed with pH2.8 drink and HFHC diet (15% fat *w/w*, 0.25% cholesterol *w/w*) until all experiments ended. All materials used in the SPF Animal Laboratory must be treated at high temperature and high pressure. All of the mice were randomly divided into four groups, baseline group (n=10), control group (n = 14), treatment group (n=14) and prevention group (n = 14). The baseline group treated with vehicle was killed after 8 weeks to evaluate the atherosclerotic lesions. The control group and the prevention group were treated with either vehicle or LXR agonist (T0901317, 10 mg/kg body weight) daily by oral gavage (0.2 mL per mouse) for 14 weeks. The treatment group was treated with vehicle for 8 weeks, and then was treated with the agonist T0901317 for additional 6 weeks. Blood samples (0.5 mL per mouse) were obtained from the retro-orbital plexus, and were centrifuged for 15 min at 4000 r/min at 4℃. Serum lipid concentrations were determined by enzymatic assays adapted to microtiter plates using commercially available reagents. All of the mice were fixed and the skin was cut from neck to abdomen. The liver and the small intestine were extracted in turn. Breastbone was cut to expose the heart. The full aorta from the root to common iliac artery was stripped. The heart and artery were taken out. Some tissues were fixed in 10% buffered neutral formalin. Others were stored in the liquid nitrogen tin.

1.5 Sudan IV staining

Aortas opened longitudinally were dehydrated with 70% alcohol for 2 min and stained using Sudan IV for 40 min, next placed in 80% alcohol for 20 min and rinsed with water for 1 h. *En face* aortic lesion areas were digitized by digital imaging system GT-800 (Seiko Epson Company) and analyzed using NIH image analysis software and expressed as the percentage of the total aortic surface area covered by lesions.

1.6 Oil red O staining

The upper portion of the heart and proximal aorta were obtained, and embedded in OCT compound at –30℃. Serial 12-μm-thick cryosections of aorta were stained with oil red O for 10 min, then rinsed for three times in distilled water for 1 min each wash. The sections were counterstained with hematoxylin, and then rinsed with 1% HCl and 70% ethanol for 1 s. Lipids accumulated in atherosclerotic plaque were observed by an optical microscope.

1.7 Paraffin sections preparation

Tissues fixed by 10% buffered neutral formalin were rinsed in distilled water for 0.5—1 h, then dipped in 70% alcohol for 24 h, 80% alcohol for 24 h, 95% alcohol I for 30 min, 95% alcohol II for 30 min, 100% alcohol I for 30 min, 100% alcohol II for 30 min, 100% alcohol and dimethylbenzene (1:1) for 20 min, dimethylbenzene I for 20 min, dimethylbenzene II for 20 min, soft wax for 10 min, and hard wax for 10 min. Paraffin mass was formed and sliced serially for 5-μm-thick every section. These sections were spread out and baked at 60℃ for 1 h, stored at room temperature.

1.8 Plasma lipid analysis

Mice were fasted overnight and euthanized. Blood samples were obtained from the retro-orbital plexus. TG, TC, HDL-C, LDL-C, ApoA-I and ApoB were determined by commercially enzymatic methods.

1.9 Real-time quantitative PCR analysis

Total RNA from aortas, livers and intestines of *apoE*$^{-/-}$ was isolated by using TRIzol reagent in accordance with the manufacturer's instructions. Reverse Transcription PCR (RT-PCR) was performed in a total volume of 20 μL at 42℃ for 60 min, using 1 μg of total RNA, 0.5 μg of oligo (dT) (15 nt), 4 μL of 25 mmol/L $MgC1_2$, 2 μL of RT-PCR buffer (10×), 2 μL of 10 mmol/L dNTP, 0.5 μL of recombinant RNasin ribonuclease inhibitor, and 15 U of AMV reverse transcriptase. Real-time quantitative PCR, using SYBR Green detection chemistry, was performed on an Applied Biosystems 7900HT Fast Real-Time PCR System. DyNAmoTM SYBR Green qPCR kit was from FINNZYMES Company. PCR amplification was performed using the specific primers (forward: 5′-TCAAG- GGAGCACGCTATGTCT-3′ and reverse: 5′-CCTCTT- CTTGCCGCTTCAGT-3′) to get the LXRα fragment (174 bp), or the specific primers (forward: 5′-TGAATG- CGGTCTCCTTGGTC-3′ and reverse: 5′-CTCACTCG- GCTTCCTTTGGTA-3′) to obtain the NPC1 fragment (109 bp). The DNA fragment was amplified using 13.5 μL deionized water, 15 μL Master Mix, 1 μL RT-PCR product, and 0.5 μL primers in a total volume of 30 μL. Melt curve analyses of all real-time PCR products were performed and shown to produce a single DNA duplex. Quantitative measurements were determined using the ΔΔ Ct method and expression of β-actin was used as the internal control.

1.10 Western blot analysis of NPC1 protein

Total aorta, liver, and small intestinal cells lysates were prepared using tissue lysis buffer containing 50 mmol/L Tris pH 8.0, 150 mmol/L NaCl, 0.02% sodium azide, 1% Nonidet P-40, 0.5% sodium deoxycholate, and 0.1% SDS supplemented with protease inhibitors[19], and centrifuged at 10000×*g* for 10 min at 4℃. The protein concentration in tissue supernatant was determined by the BCA assay. Equal amounts of proteins (typically 50 μg) were separated on 8% SDS-PAGE gel and electrophoretically transferred to NC membranes. Each blot was visualized for protein using Ponceau S and the position of the molecular mass standard was determined. After being blocked with 5% nonfat milk for 2 h, the transferred NC membranes were incubated overnight with a goat monoclonal antibody to mouse NPC1 at a dilution of 1:500 on a rotating platform at 4℃. Subsequently, membranes were rinsed 3 times in TBST (pH 7.6) and incubated with horseradish peroxidase-conjugated anti-goat IgG antibodies diluted in TBST (1:7000) for 1 h on a rotating platform at 4℃. The membranes were rinsed 3 times again in TBST (pH 7.6). The signal was visualized by enhanced chemiluminescence according to the manufacturer's recommendation. The films were scanned with the Labwork software. The area of protein bands in the experiment groups was compared and semi-quantitatively analyzed with that of the control group which was set as 100%.

1.11 Immunohistochemistry

Five-μm-thick consecutive sections were cut from 10% formalin-fixed and paraffin-embedded tissue blocks. Sections were de-waxed in xylene and rehydrated through graded concentrations of ethanol to distilled water. Sections were then immersed in 10 mmol/L citrate buffer (pH 6.0) and processed in a thermostatic water bath for antigen retrieval. Immunohistochemistry was performed according to a slightly modified SABC (stretavidin–biotin–peroxidase complex) method with 3-3′ diaminobenzidine tetrahydrochloride (DAB) development. The sections were counterstained with haematoxylin, dehydrated, differentiated and mounted with permanent mounting medium. Tissues were examined with an optical microscope. Negative control sections were stained with PBS. Antigen showed diffused staining of which density and distribution were not homogeneous. The cells expressing NPC1 protein were identified by dark-brown or brown-yellow nuclear staining.

1.12 Cell culture

THP-1 cells were maintained in RPMI 1640 containing 10% fetal bovine serum in a 5% CO_2 incubator at 37℃. 1.0×10^5 IU/L penicillin-streptomycin antibiotic solution was added to culture medium. Differentiation of THP-1 monocytes into macrophages was induced by plating the cells at a density of 1.0×10^6 cells/well in a six-well plate in the presence of 160 nmol/L PMA for 24 h and then used for the experiments[20].

1.13 siRNA sequences design, vectors construction and transfection

Using GenBank sequence for human *NPC1* cDNA and computer analysis software developed by Ambion Company, we designed and synthesized specific DNA complementary oligonucleotides (sense strand: 5′-CCAGGUUCUUGACUUACAAUU-3′, antisense strand: 5′-UUGUAAGUCAAGAACCUGGUU-3′) based on the

coding region sequences (NNCCAGGUUCUUGACUUACAA) of human *NPC1* cDNA. In addition, a pair of DNA oligonucleotides that have not any homology with human *NPC1* sequences were used as the negative control. One μg of each single-strand DNA synthesized segment was incubated in annealing buffer at 95℃ for 4 min. The reaction mixture was cooled to room temperature gradually. Single-strand DNA oligonucleotides turned into double-strand DNA after anneal. The double-strand DNA was ^{32}P-labeled by using [γ-^{32}P]ATP and treated with T4 polynucleotide kinase. The annealed double-strand DNA for siRNA was ligated with linearized p*Silencer* 2.1-U6 siRNA expression vector at *Bam*H I and *Hin*d III sites. The products were transformed into competent *Escherichia coli* DH5α cells and cultured on Luria-Bertani (LB) plates with 100 μg/mL ampicillin. Ampicillin-resistant colonies were selected by restriction digestion and confirmed by DNA sequencing. The THP-1 macrophages were transfected using Lipofectamine^{TM} 2000 reagent according to the manufacturer's protocol. All cells were propagated in Dulbecco's Modified Eagle's Medium (DMEM) without serum and antibiotics during the transfection. After 6—12 h of incubation in a CO_2 incubator, the medium was replaced by fresh medium containing serum and antibiotics until 72 h after transfection. The efficiency of *NPC1* gene silencing was evaluated by real-time quantitative PCR and Western blot analyses.

1.14 Assessment of cholesterol efflux

THP-1 macrophages were incubated in fresh growth RPMI1640 medium supplemented with 0.2 mCi/L [^{3}H]-cholesterol and 10% calf serum.

THP-1 macrophages were subjected to different treatments:

(1) Normal control: The cells were cholesterol-loaded using 50 mg/L oxidized LDL.

(2) SiRNA: *NPC1* gene-silenced cells were cholesterol-loaded using 50 mg/L oxidized LDL.

(3) LXR agonist: Cells were treated with T0901317 and cholesterol-loaded using 50 mg/L oxidized LDL.

(4) SiRNA and LXR agonist: THP-1 cells were simultaneously treated with siRNA and T0901317 together with cholesterol-loaded using 50 mg/L oxidized LDL.

After 48 h of incubation, each group of cells was washed with phosphate-buffered saline (PBS) and incubated with RPMI1640 medium containing 2 g/L bovine serum albumin for additional 24 h. All of the cells were washed again with PBS and incubated in serum-free medium containing 10 mg/L apoA-I for 12 h. [^{3}H]-cholesterol in culture medium and cell was determined by FJ-2107P type liquid scintillator. Cholesterol efflux is expressed as a percentage, calculated as [^{3}H]-cholesterol in medium/([^{3}H]-cholesterol in medium+[^{3}H]-cholesterol in cells)×100%[20].

1.15 Statistical analysis

Data are expressed as means±S.D. Results were analyzed by one-way ANOVA and Student's *t* test, using SPSS 11.0 software. Statistical significance was obtained when *P* values were less than 0.05.

2 Results

2.1 Analysis of atherosclerosis in *en face* mouse aortic preparations by Sudan IV staining

To investigate whether T0901317 exerts a preventive and reversal effect on atherosclerosis, we determined the atherosclerotic lesion area by Sudan IV staining. The percentage of the total aortic surface area occupied by lesions was then calculated. The percentage of the baseline group, control group, prevention group and treatment group is (10.8±1.2)%, (15.1±1.7)%, (5.4±0.6)% and (6.3±0.8)%, respectively. LXR agonist treatment resulted in a 64.2% and 58.3% reduction of aortic atherosclerotic lesion area in the prevention group and treatment group, respectively, compared with controls (P<0.01, Figure 1), demonstrating a preventive and reversal effect of the LXR agonist on lesion development. Furthermore, LXR agonist resulted in a significant 41.7% reduction in lesion areas in the treatment group compared with the mice assessed in the baseline group (P<0.05, Figure 1), demonstrating that the LXR agonist induced regression of established atherosclerotic lesions.

2.2 Analysis of atherosclerosis in aortic root transverse section by oil red O staining

The basal portion of the heart and proximal aorta in *apoE*$^{-/-}$ mice was frozen on dry ice and sectioned. Serial transverse sections of the aortic root were stained with oil red O to allow quantification of the extent of the atherosclerotic lesions. The percentage of total aortic lumen occupied by lesions per section was then calculated. The percentage of the baseline group, control group, prevention group and treatment group is (21.9 ±

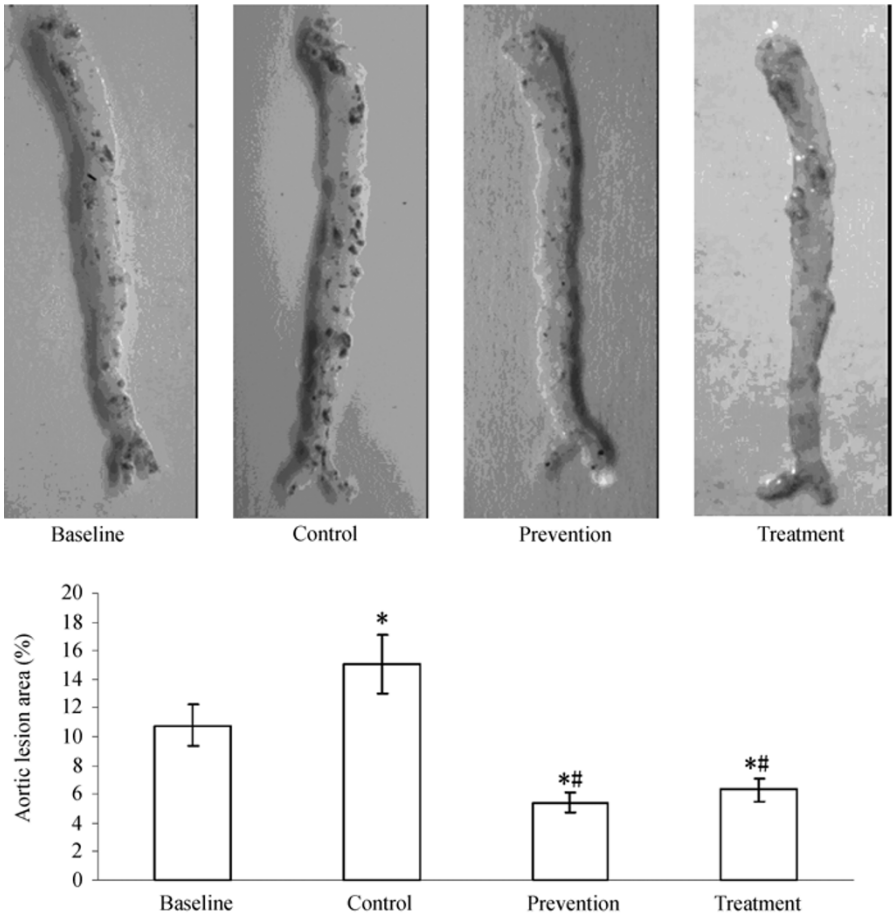

Figure 1 Effect of T0901317 on atherosclerotic lesions in aorta of $apoE^{-/-}$ mice (n=3). *, P<0.05 vs Baseline; #, P<0.01 vs Conrol.

2.1)%, (29.7±3.2)%, (7.8±0.8)% and (8.9±0.9)%, respectively. These data revealed a statistically significant 73.7% and 70.0% reduction in aortic root atherosclerotic lesion area in the prevention group and treatment group, respectively, compared with the vehicle-treated controls (P<0.01, Figure 2).

2.3 Examination of plasma lipid concentrations in *apoE*$^{-/-}$ mice

Because LXRs are involved in regulation of cholesterol and lipid metabolism, we examined the terminal plasma lipid levels from experimental mice. As shown in Table 1, treatment of $apoE^{-/-}$ mice fed with a HFHC diet with T0901317 led to an 80% to 95% increase in plasma TG levels. A modest 28.9% to 34.7% increase in TC was accompanied by a 72.5% to 76.7% increase in HDL-C. However, no significant alternation occurred in LDL-C. ApoA-I was also elevated. No difference occurred in body weight between groups at the end of the experiments.

2.4 Effect of T0901317 on LXRα and *NPC1* gene expression in the liver, aorta and small intestine of *apoE*$^{-/-}$ mice

To observe the effect of T0901317 on LXRα and *NPC1* mRNA expression, we collected the liver, small intestine and aorta of $apoE^{-/-}$ mice to perform real-time quantitative PCR. Our data suggested that *LXRα* and *NPC1* mRNA expression in these tissues of T0901317-treated $apoE^{-/-}$ mice was significantly increased, compared with vehicle-treated controls (P<0.05, Figures 3 and 4).

2.5 Effect of T0901317 on NPC1 protein levels in the liver, aorta and small intestine of *apoE*$^{-/-}$ mice

To examine the NPC1 protein levels, we further performed Western blot analysis and immunohistochemistry. Immunohistochemistry analysis showed that brown or brown coloring cells in the small intestine, liver and aorta slices of the treatment group and the prevention group were significantly more than those in the control group. Western blotting results indicated that *NPC1* lev-

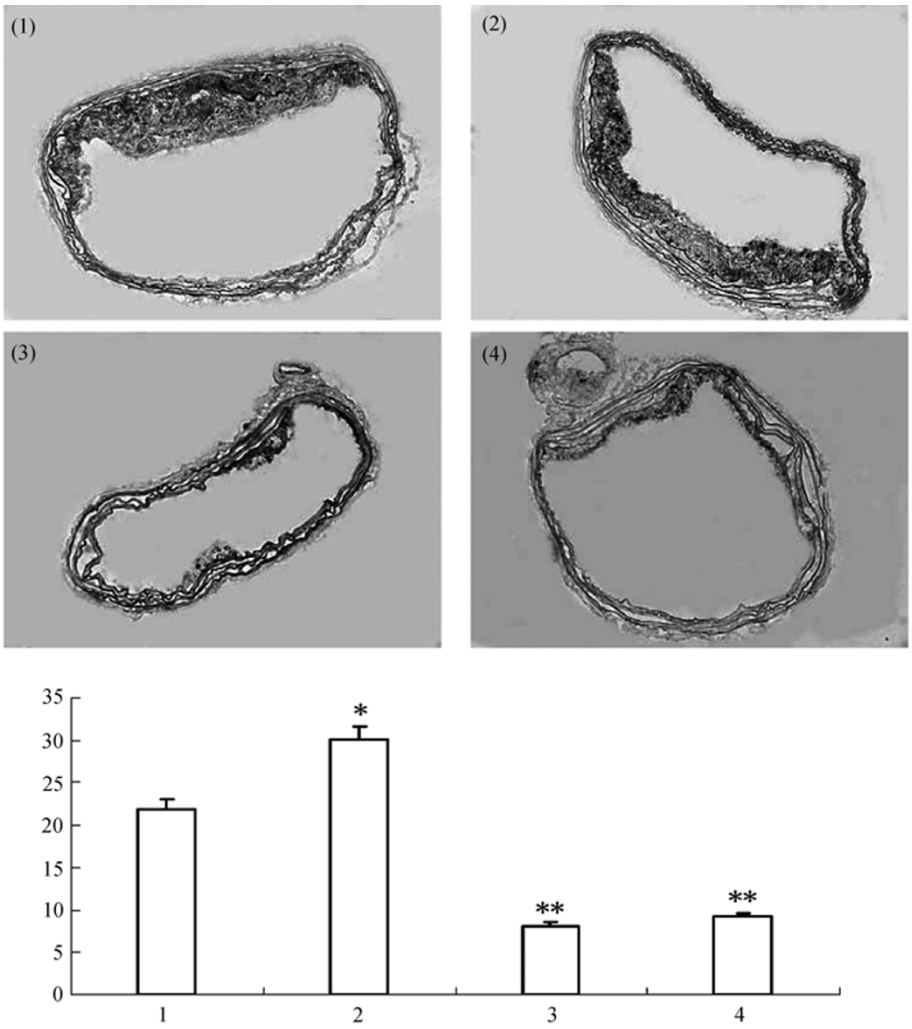

Figure 2 Analysis of atherosclerotic lesion area in aortic root transverse section (×10, n=3). 1, Baseline; 2, Control; 3, Prevention; 4, Treatment. *, P<0.05 vs Baseline, **, P<0.01 vs Baseline and vs Control.

Table 1 Terminal plasma lipid levels in $apoE^{-/-}$ mice fed with a HFHC diet (Mean±SD)

	Baseline (n=10)	Control (n=14)	Prevention (n=14)	Treatment (n=14)
Body weight (g)	30.10 ± 3.27	30.13 ± 3.42	29.19 ± 2.89	28.86 ± 3.13
TG (mmol/L)	1.21 ± 0.21	1.20 ± 0.24	2.34 ± 0.27**	2.16 ± 0.23**
TC (mmol/L)	27.71 ± 3.03	29.13 ± 3.37	39.25 ± 4.71*	37.55 ± 4.22*
HDL-C (mmol/L)	11.32 ± 1.41	10.65 ± 1.32	18.82 ± 1.96**	18.37 ± 1.84**
LDL-C (mmol/L)	16.28 ± 1.90	18.44 ± 1.96	20.40 ± 2.98	19.17 ± 2.34
ApoA-I (g/L)	0.03 ± 0.00	0.03 ± 0.00	0.05 ± 0.01*	0.04 ± 0.00*
ApoB (g/L)	0.13 ± 0.02	0.13 ± 0.02	0.14 ± 0.02	0.13 ± 0.02
ApoA- I /ApoB	0.23 ± 0.03	0.23 ± 0.03	0.36 ± 0.03**	0.31 ± 0.03**

TG, triglyceride; TC, total cholesterol; HDL-C, high density lipoprotein-cholesterol; ApoA-I, apolipoprotein A-I; ApoB, apolipoprotein B. *, P<0.01 vs Control; **, P<0.005 vs Control.

els were significantly increased in the aorta, liver and small intestine of $apoE^{-/-}$ mice treated with T0901317, compared with the control group (P<0.05, Figures 5 and 6). These results are consistent with the data from real-time quantitative PCR analysis. All protein levels were assessed by densitometry with β-actin as a control.

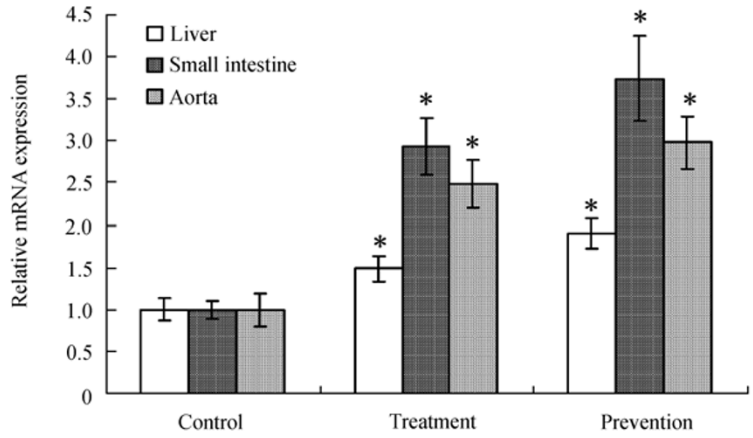

Figure 3 Regulation of *LXRα* mRNA expression by T0901317 in the liver, small intestine and aorta of *apoE*$^{-/-}$ mice (n=3). *, P<0.05 vs Control.

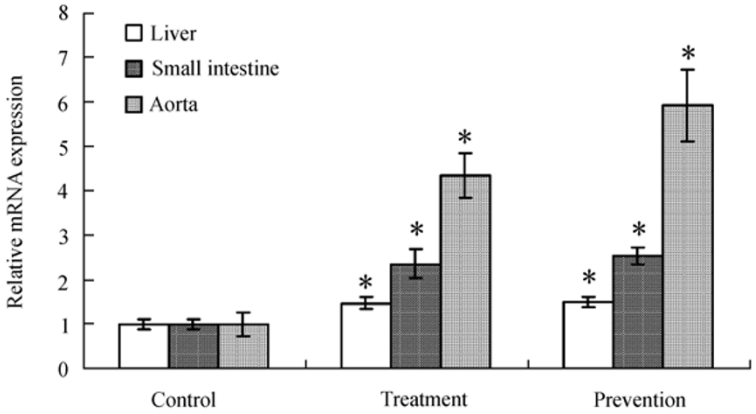

Figure 4 Regulation of *NPC1* mRNA expression by T0901317 in the liver, small intestine and aorta of *apoE*$^{-/-}$ mice (n=3). *, P<0.05 vs Control.

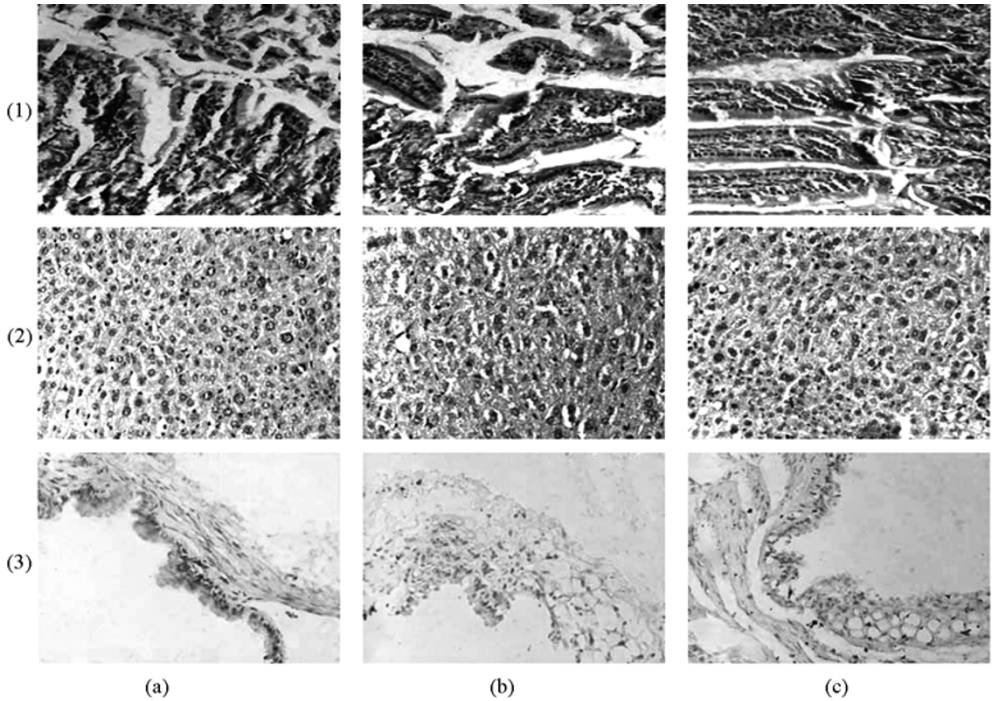

Figure 5 NPC1 protein levels in *apoE*$^{-/-}$ mice determined by immunohistochemisty (×40, n=3). (1) Small intestine; (2) Liver; (3) Aorta. (a) Control; (b) Treatment; (c) Prevention.

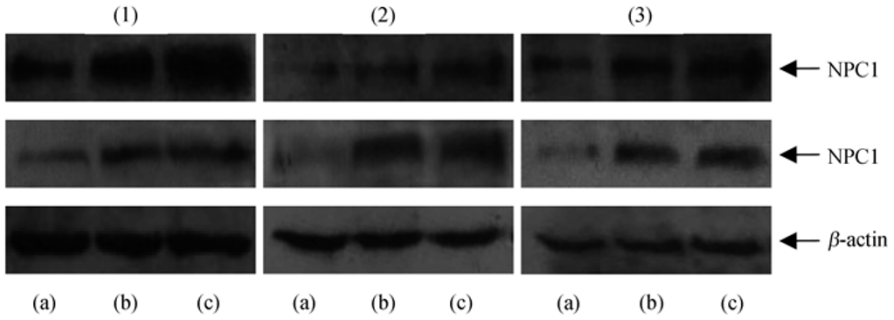

Figure 6 NPC1 protein levels in *apoE*$^{-/-}$ mice determined by Western blotting (n=2). (1) Liver; (2) Small intestine; (3) Aorta. (a) Control; (b) Treatment; (c) Prevention.

2.6 *NPC1* mRNA and protein expression in *NPC1* siRNA-transfected cells

In order to observe the efficiency of siRNA transfection into the cells, we detected *NPC1* mRNA expression in normal control, negative control, and siRNA THP-1 macrophage-derived foam cells using real-time quantitative PCR. The data showed that *NPC1* mRNA relative expression in normal control cells was almost consistent with that of negative control cells, however that of siRNA cells was reduced by 71%, compared with the negative control cells (P<0.05, Figure 7).

To estimate the efficiency of siRNA transfection into the cells, we also detected NPC1 protein levels in THP-1 macrophage-derived foam cells by Western blotting. The data showed that NPC1 protein levels were almost equal between normal control cells and negative control cells, whereas NPC1 protein levels in siRNA THP-1 macrophage-derived foam cells were significantly reduced, compared with the negative control cells (P<0.05, Figure 8), which indicates RNA interference markedly decreased NPC1 protein levels in THP-1 macrophage-derived foam cells.

2.7 Effect of T0901317 on cholesterol efflux in *NPC1* gene silenced THP-1 macrophage-derived foam cells

To determine the effect of T0901317 on cholesterol efflux, we used RNA interference technology to silence *NPC1* gene expression in THP-1 macrophage-derived foam cells. The results showed that the rate of cholesterol efflux in four group cells was 8.1%, 2.9%, 17.8% and 9.9%, respectively (Figure 9). Compared with the normal cells, cholesterol efflux of siRNA THP-1 macrophage-derived foam cells was significantly decreased (P<0.05), whereas cholesterol efflux of LXR agonist T0901317-treated THP-1 macrophage-derived foam cells was significantly increased (P<0.05). No significant difference of cholesterol efflux occurred between siRNA THP-1 macrophage-derived foam cells treated with T0901317 and normal control cells. Compared with LXR agonist T0901317-treated THP-1 macrophage-derived foam cells, cholesterol efflux in siRNA and LXR agonist T0901317-treated THP-1 macrophage-derived foam cells was significantly decreased (P<0.01). These results suggest that NPC1 plays a certain role in LXR-mediated cholesterol efflux.

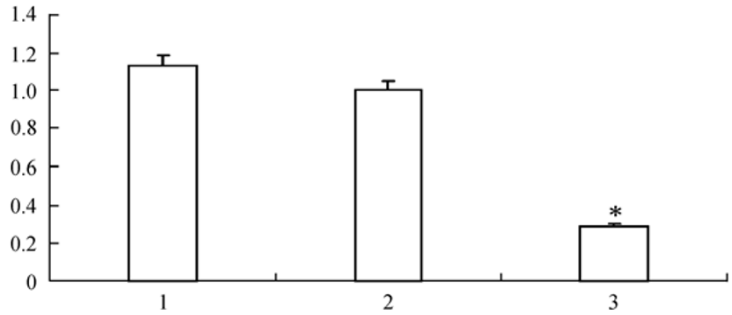

Figure 7 Effect of RNA interference on *NPC1* mRNA expression in THP-1 macrophage-derived foam cells (n=3). 1, Normal control; 2, Negative control; 3, siRNA. *, P <0.05 vs Negative control group.

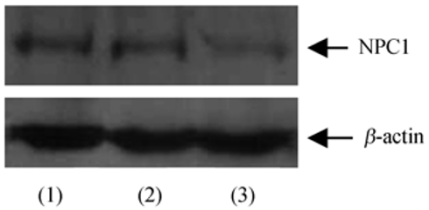

Figure 8 Effect of RNA interference on NPC1 protein levels in THP-1 macrophage-derived foam cells (n= 3). (1) Normal control; (2) Negative control; (3) siRNA.

3 Discussion

LXRs (LXRα and LXRβ) are sterol-activated transcription factors that belong to the nuclear receptor family and play a critical role in cholesterol homeostasis and bile acid metabolism[21]. LXRα is mainly expressed in the liver, adipose tissue, small intestine, kidney and macrophages, while LXRβ is ubiquitously expressed in many cell types[22]. In the liver, LXRs increase bile acid synthesis through inducing cholesterol 7α-hydroxylase gene expression and promoting cholesterol efflux from the hepatocytes. In the small intestine, LXR activation promotes cholesterol efflux from small intestine cells and reduces cholesterol absorption through the activation of ABCA1 expression[23]. In macrophages, LXRs increase ABCA1 expression and promote ApoA-I mediated cholesterol efflux[15]. NPC1 transfers cholesterol in late endosome (LE)/lysosome (LY) to the cell membrane. The cholesterol in LE/LY is a priority as ABCA1-mediated cholesterol efflux[24]. Therefore, NPC1 may promote cholesterol efflux from macrophages through transporting cholesterol in LE/LY to the cell membrane and prevent the macrophages transforming into foam cells.

In this study, the data suggested LXR agonist T0901317 not only inhibited the initiation of atherogenesis but induced regression of preexisting atherosclerotic lesions. T0901317 induced both *NPC1* and *LXRα* gene and protein expression in atherogenic $apoE^{-/-}$ mice. Furthermore, our results demonstrated that plasma TG, TC, HDL-C and apoA-I concentrations were markedly increased in T0901317-treated groups.

A previous study showed that mice lack of LXRα and LXRβ had severe atherosclerotic lesions compared with the wild-type mice and the transfer of bone marrow transplantation from LXRαβ double knockout mice to apoE and LDLR double knockout mice results in a increase in atherosclerosis in these mice[25]. Sean et al suggested LXR synthetic ligands inhibited atherosclerosis development in apoE and LDLR double knockout mice[26]. LXR agonist GW3965 reduced 47% of the atherosclerotic lesion area in the $apoE^{-/-}$ mice[26,27]. Our results showed T0901317 reduced atherosclerotic lesions in the $apoE^{-/-}$ mice fed with HFHC diet.

LXR synthetic agonists GW3965 and T0901317 increased LXRα expression in differentiated THP-1 cells, but had not any significant effect on the LXRβ expression[28]. Another study indicated T0901317 significantly induced the expression of LXRα gene in adipose tissue of mouse and human[29]. We determined the LXRα mRNA expression and found that T0901317 upregulated the expression of LXRα mRNA in the liver, aorta and small intestine of $apoE^{-/-}$ mice.

In the presence of progesterone (it prevents cholesterol from LE/LY mobilization to the membrane and simulates the NPC phenotype), the cholesterol in cell membrane of macrophages was significantly reduced and apoA-I-mediated cholesterol efflux induced by LXR agonist was markedly blocked. LXR activation enhances cholesterol trafficking to the plasma membrane, where it becomes available for efflux, at the expense of esterification, thus contributing to the overall effects of LXR

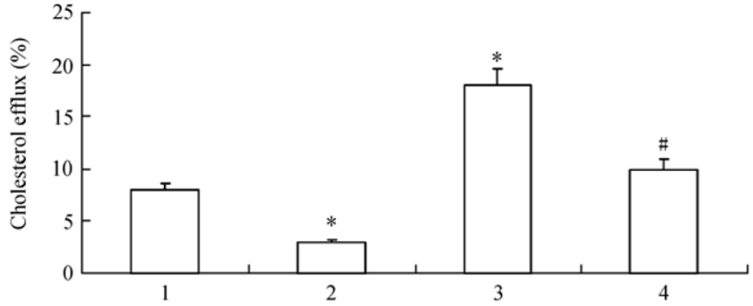

Figure 9 Effect of *NPC1* gene silencing on cholesterol efflux from THP-1 macrophage-derived foam cells (n=3). 1, Normal control; 2, siRNA; 3, LXR agonist; 4, siRNA and LXR agonist. *, P<0.05 vs Normal group; #, P<0.01 vs siRNA and LXR agonist.

agonists in the control of macrophage cholesterol homeostasis[12]. ABCA1 gene expression was down-regulated in human fibroblasts of *NPC1* gene deficiency, but T0901317 significantly increased ABCA1 gene expression and protein activity and promoted cholesterol efflux from these cells to ApoA-I[30]. The above results indicate LXR activation regulates both ABCA1 and NPC1.

Our results showed T0901317 increased *NPC1* expression in the liver, small intestine and aorta of $apoE^{-/-}$ mice fed with a HFHC diet, which indicates NPC1 may contribute to reduction of atherosclerotic lesions. $NPC1^{-/-}$ mice were crossed with $apoE^{-/-}$ mice to examine the effect of NPC1 on atherosclerotic lesion formation and the double-mutant mice showed a greater lesion area compared with $apoE^{-/-}$ littermates[31], which indicated knockout of *NPC1* gene increases atherosclerosis. We silenced the *NPC1* gene expression of THP-1 macrophages using RNA interference technology, then induced macrophages to become foam cells and observed the effect of T0901317 on cholesterol efflux in THP-1 macrophage-derived foam cells. Our results showed that T0901317 promoted cholesterol efflux and *NPC1* gene silencing significantly reduced cholesterol efflux in the presence or absence of T0901317, which indicated that NPC1 plays an important role in intracellular cholesterol efflux. Previous studies have demonstrated that addition of T0901317 to human $NPC1^{-/-}$ fibroblasts raised cholesterol efflux to apoA-I to the levels similar to only 42% of levels in apoA-I-plus LXR agonist-treated $NPC1^{+/+}$ cells, but to the levels similar to those in apoA-I-treated $NPC1^{+/+}$ cells[30], which indicates that T0901317 elevates cellular cholesterol efflux though inducing *NPC1* expression. Consistent with the previous study, our results further demonstrated T0901317 alleviate atherosclerosis in $apoE^{-/-}$ mice through promoting *NPC1* gene expression and protein levels.

LXR agonist increased plasma levels of HDL-C through increasing the expression of ABCA1, apoE and phosphate transfer protein (PLTP)[32]. However, mutations in *NPC1* impair the regulation and activity of ABCA1, resulting in decreased efflux of cell phospholipids and cholesterol and formation of HDL particles *in vitro*, and low plasma HDL levels in the majority of NPC patients[33], which indicates NPC1 play a key role in HDL formation. Our results showed that LXR agonist T0901317 increased plasma HDL-C levels in $apoE^{-/-}$ mice. We consider that T0901317 promotes cholesterol efflux from peripheral cells in $apoE^{-/-}$ mice to apoA-I acceptor by inducing NPC1 and ABCA1 expression, thus increasing the plasma HDL-C levels. So, regulation of *NPC1* by LXR plays a vital role in control of plasma HDL levels.

Plasma HDL cholesterol levels are negatively related to cardiovascular disease events[34]. Although LXR activation increases the plasma levels of HDL, it promotes the TG synthesis and leads to hyperlipidemia, which is an independent risk factor of atherosclerosis. LXRs regulate fatty acid synthesis in the liver through control of sterol regulatory element binding protein-1c (SREBP-1c), acetyl-CoA carboxylase (ACC), fatty acid synthase (FAS) and stearoyl-CoA desaturase-1 (SCD-1)[35]. SREBP-1c plays an important role in LXR-mediated fatty acid synthesis by activating an array of genes involved in fatty acid metabolism[36].

In conclusion, our study showed that LXR agonist T0901317 not only inhibited atherosclerosis development but also increased the expression of NPC1 in liver, small intestine and aorta of $apoE^{-/-}$ mice. *NPC1* gene silencing reduced cellular cholesterol efflux from THP-1 macrophage-derived foam cells. These results suggest that NPC1 plays an important role in the development of atherosclerosis.

1 Ira T. Cholesterol and phospholipids metabolism in macrophages. Biochim Biophys Acta, 2000, 1529(1-3): 164－174

2 Tang C K, Yi G H, Yang J H, et al. Oxidized LDL upregulated ATP binding cassette transporter-1 in THP-1 macrophages. Acta Pharmacol Sin, 2004, 25(5): 581－586

3 Jessica P, Laura L. Flux of fatty acids through NPC1 lysosomes. J Biol Chem, 2005, 280(11): 10333－10339

4 Yuki O, Yuko S, Michitaka S, et al. Cholesterol depletion facilitates ubiquitylation of NPC1 and its association with SKD1/Vps4. Cell Sci, 2006, 119(13): 2643－2653

5 Ou X, Tang C K. Roles of NPC1 and NPC2 in intracellular lipid homeostasis. Chin J Pathophysiol (in Chinese), 2007, 23(4): 820－824

6 Nobutaka O, Dennis C K, Matthew T, et al. Binding between the Niemann–Pick C1 protein and a photoactivatable cholesterol analog requires a functional sterol-sensing domain. Proc Natl Acad Sci USA, 2004, 101(34): 12473－12478

7 John M D, Stephen D T. Control of cholesterol turnover in the mouse. J Biol Chem, 2002, 277(6): 3801－3804

8 Stacie K L, Jill A M, Eugene D C, et al. Murine model of Niemann–Pick C disease: Mutation in a cholesterol homeostasis gene. Science, 1997, 277(5323): 232－235

9 Laura L. Niemann-Pick type C mutations cause lipid traffic jam. Traffic, 2000, 1(3): 218－225

10 Catherine S, Maureen E H, Joanna P D, et al. Targeting of NPC1 to late endosomes involves multiple signals, including one residing within the putative sterol-sensing domain. J Biol Chem, 2004, 279(46): 48214－48223
11 Cheruku S R, Zhi X, Roxanne D, et al. Mechanism of cholesterol transfer from the Niemann-Pick type C2 protein to model membranes supports a role in lysosomal cholesterol transport. J Biol Chem, 2006, 281(42): 31594－31604
12 Rigamonti E, Helin L, Lestavel S, et al. Liver X receptor activation controls intracellular cholesterol trafficking and esterification in human macrophages. Circ Res, 2005, 97(7): 682－689
13 Chen D Y, Jeffrey G M, Patel A, et al. Sterol intermediates from cholesterol biosynthetic pathway as liver X receptor ligands. J Biol Chem, 2006, 281(38): 27816－27826
14 Tang C K, Xi S M, Yin W D, et al. Change of ATP binding cassette transporter A1 expression in diabetic minipigs. Prog Biochem Biophys (in Chinese), 2004, 31(6): 543－549
15 Asha V, Bryan A L, Sean B J, et al. Control of cellular cholesterol efflux by the nuclear oxysterol receptor LXRalpha. Proc Natl Acad Sci USA, 2000, 97(22): 12097－12102
16 Bradley M N, Hong C, Chen M, et al. Ligand activation of LXRß reverses atherosclerosis and cellular cholesterol overload in mice lacking LXRα and apoE. J Clin Invest, 2007, 117(8): 2337－2346
17 Toshimori I, Morihiro M, Mitsuru S, et al. Angiopoietin-like protein 3 mediates hypertriglyceridemia induced by the liver X receptor. J Biol Chem, 2003, 278(24): 21344－21351
18 Choe S S, Choi A H, Lee J W, et al. Chronic activation of liver X receptor induces ß-cell apoptosis through hyperactivation of lipogenesis, liver X receptor–mediated lipotoxicity in pancreatic ß-cells. Diabetes, 2007, 56(6): 1534－1543
19 Tang C K, Tang G H, Yi G H, et al. Effect of apolipoprotein A-I on ATP binding cassette transporter A1 degradation and cholesterol efflux in THP-1 macrophage-derived foam cells. Acta Biochim Biophys Sin, 2004, 36(3): 218－226
20 Tang C K, Yang J H, Yi G H, et al. Effects of oleate on ATP binding cassette transporter A1 expression and cholesterol efflux in THP-1 macrophage derived foam cell. Acta Biochim Biophys Sin (in Chinese), 2003, 35(12): 1077－1082
21 Cha J Y, Repa J J. The liver X receptor (LXR) and hepatic lipogenesis: The carbohydrate-response element-binding protein is a target gene of LXR. J Biol Chem, 2007, 282(1): 743－751
22 Emi K, Morihiro M, Yukio Y, et al. Induction of intestinal ATP-binding cassette transporters by a phytosterol-derived liver X receptor agonist. J Biol Chem, 2003, 278(38): 36091－36098
23 Dai X Y, Ou X, Hao X R, et al. A synthetic LXR agonist T0901317 inhibits semicarbazide-sensitive amine oxidase gene expression and activity in *apoE*$^{-/-}$ mice. Acta Biochim Biophys Sin, 2008, 40(3): 261－268
24 Wengen C, Yu S, Carrie W, et al. Preferential ATP-binding cassette transporter A1-mediated cholesterol efflux from late Endosomes/Lysosomes. J Biol Chem, 2001, 276(47): 43564－43569
25 Rajendra K T, Eric D B, Sean B J, et al. Identification of macrophage liver X receptors as inhibitors of atherosclerosis. Proc Natl Acad Sci USA, 2002, 99(18): 11896－11901
26 Sean B J, Elaine M, Liming P, et al. Synthetic LXR ligand inhibits the development of atherosclerosis in mice. Proc Natl Acad Sci USA, 2002, 99(11): 7604－7609
27 Bruemmer D, Law R E. Liver X Receptors: Potential novel targets in cardiovascular diseases. Current Drug Targets—Cardiovascular & Haematological Disorders, 2005, 5(6): 533－540
28 Whitney K D, Watson M A, Goodwin B, et al. Liver X receptor regulation of the LXRα gene in human macrophages. J Biol Chem, 2001, 276(47): 43509－43515
29 Ulven S M, Dalen K T, Gustafsson J A, et al. Tissue-specific autoregulation of the LXRα gene facilitates induction of apoE in mouse adipose tissue. J Lipid Res, 2004, 45(11): 2052－2062
30 Boadu E, Choi H Y, Lee D W K, et al. Correction of apolipoprotein A-I-mediated lipid efflux and high density lipoprotein particle formation in human Niemann-Pick type C disease fibroblasts. J Biol Chem, 2006, 281(48): 37081－37090
31 Welch C L, Sun Y, Arey B J, et al. Spontaneous atherothrombosis and medial degradation in *apoE*$^{-/-}$, *npc1*$^{-/-}$ mice. Circulation, 2007, 116(21): 2444－2452
32 Jiang X C, Thomas P B, Li Z Q, et al. Enlargement of high density lipoprotein in mice via liver X receptor activation requires apolipoprotein E and is abolished by cholesteryl ester transfer protein expression. J Biol Chem, 2003, 278(49): 49072－49078
33 Hong Y C, Barbara K, Teddy C, et al. Impaired ABCA1-dependent lipid efflux and hypoalphalipoproteinemia in human Niemann-Pick type C disease. J Biol Chem, 2003, 278(35): 32569－32577
34 Dai X Y, Ou X, Hao X R, et al. Effect of T0901317 on hepatic proinflammatory gene expression in *apoE*$^{-/-}$ mice fed a high-fat/high- cholesterol diet. Inflammation, 2007, 30 (3-4): 105－117
35 Peter T, David J M. Liver X receptor signaling pathways in cardiovascular disease. Mol Endocrinol, 2003, 17(6): 985－993
36 Joshua R S, Tu H, Alvin L, et al. Role of LXRs in control of lipogenesis. Genes Dev, 2000, 14(22): 2831－2838